

## Chapter 2

# Modeling for the Analysis of the EDA

As described in the previous chapter, EDA broadly refers to any alterations in the electrical properties of the skin. The most frequently used measure of EDA is the SC. The SC signal can be decomposed in two components, tonic and phasic, which have different time scales and relationships to exogenous stimuli. Tonic phenomena include slow drifts of the baseline skin conductance level (SCL) and spontaneous fluctuations (SF) in SC [15]. The phasic component, i.e., the skin conductance response (SCR), reflects the short-time response to the stimulus. The typical shape of SCR is comprised of a relatively rapid rise from the conductance level followed by a slower, asymptotic exponential decay back to the baseline.

When the inter-stimulus interval (ISI), i.e., the temporal gap between two consecutive stimuli, is shorter than the recovery time of the first response, the two SCRs overlap. This occurrence is observed in many experimental paradigms, particularly in cognitive neuroscience where common values of ISI (1–2 s) are generally shorter than the recommended minimum ISI to avoid such an overlap, which is around 10–20 s [17, 61]. The overlap issue is probably the main limitation in the treatment of the decomposition of SC into its phasic and tonic components. Despite the wide use of EDA measurements and related research, the generation of SCR via skin sympathetic nerve fibres is still unknown.

### 2.1 Mathematical Models of the EDA: An Overview

In the past two decades, several mathematical solutions have been developed to decompose the phasic signal into individual SCRs associated with each stimulus, even during short ISI experimental paradigms, and to model how ANS activity (and, in particular, the sudomotor nerve activity) causes SCRs. This process allows estimation of ANS activity with potentially better time resolution than using the raw SCR signal. Many of the early methods, whose primary aim was to overcome

the overlap issue, required visual inspection and introduced subjective elements into the analysis. For example, Barry et al. [62] attempted to correct the baseline by subtracting each SCR from an extension of the preceding SCR using graphical tools. Lim et al. [63] proposed a model based on a response function made of 4–8 parameters optimized for each single response to obtain a response-by-response variation in SCR shape. This method also required visual inspection to select the best model setting.

Further assumptions have been related to the description of the peripheral nervous system as a linear time-invariant (LTI) system [64]. In addition to decomposing the phasic signal into individual SCRs, these models often attempt to estimate the ANS activity by searching for the most likely input signal which could explain the observed output (the measured SC). The first LTI model for EDA analysis was presented by Alexander et al. [65]. Their method allowed the estimation of the sudomotor nerve activity (SMNA) using a model where the SC is the result of a convolution between discrete bursting episodes of the SMNA and a biexponential impulse response function (IRF) assumed to be known a priori and time invariant.

Benedek and Kaernbach criticized some aspects of Alexander’s model and developed two new models in which the LTI assumption was modified to take into account the variability in SCR shape. In addition, they considered mathematical constraints to significantly improve the reliability of the physiological modeling. These models are known as the non-negative deconvolution model [16] and the continuous deconvolution model [1]. Both models split the SMNA into two parts, one describing the actual phasic activity and the other representing EDA variations of different origins (e.g., noise). Both models assume a pharmacokinetic model of the dynamic law of diffusion of sweat. They adopted a biexponential IRF, called the Bateman function. Although observation noise is not formally modeled in any of these methods [1, 16, 65], all of three assume its existence. They estimate a noisy SMNA and then recover a filtered phasic component using a low-pass filter and a subsequent heuristic and prefixed peak-detection scheme.

Recently, Bach et al. presented the SCRalyze toolbox (now incorporated into PsPM and available online at: [pspm.sourceforge.net](http://pspm.sourceforge.net)), which comprises several models that assume a linear time-invariant system [66]. Note that Bach’s model also imposes mathematical constraints to improve the physiological mimicking. These models and that of Alexander et al. use a heuristic IRF whose parameters have been optimized on large datasets. SCRalyze algorithms try to estimate the model input (SMNA) or parameters that best explain the observed SC data based on optimization methods. Moreover, they include a noise term, which also accounts for possible violations of the assumption of time invariance.

More recently, Chaspari et al. [67] proposed a sparse representation of EDA but their use of overcomplete dictionaries leads to a non-convex problem with no guarantee of finding the globally optimal solution. Since a great variety of practical problems can be cast in the form of a convex optimization problem, mathematical optimization has become an important tool in many disciplines and the list of its applications is steadily growing [68].

In this book, we report on a recently proposed method called CvxEDA [69] to estimate the ANS activity from the EDA using a convex optimization approach. The model is grounded on Bayesian statistics and a simple yet physiologically sound representation of the observed SC as the sum of three components: a slow tonic component; the output of the convolution between an IRF and a sparse (compact, bursty) non-negative SMNA phasic driver; and an additive noise term. Of note, the IRF, which is related to the phasic component, is modeled as output of an Infinite Impulse Response (IIR) system.

## 2.2 EDA Analysis

EDA is a widely used measurement in, e.g., the psychophysiology research field. In this context, one of the main goal is to infer on perceptual affective states from physiological, peripheral, may be non-invasive measurements such as SCR. However, sometimes psycho-physiological processes (e.g., sympathetic arousal) can have higher time resolution than the observed variables (e.g., SCRs). This shortcoming dramatically impact on the use of conventional analysis, which does not employ any a-priori modeling. Consequently, recent years have seen an increased interest in the design of causal models, aiming to estimating unobservable processes from observable ones such that inference can be drawn from the unobservable variable directly [64, 66].

In the following text, we take into account two different approaches: the conventional and the model-based approach.

### 2.2.1 *Conventional Analysis*

The aim of conventional analysis is to extract features from the observable variable, in this case the SC signal, that can closely represent a psychological central state. A conventional data analysis algorithm can be described as follows: (1) data filtering to reduce the observation noise, (2) definition of a time response window in order to identify only the peaks that are stimulus-evoked, and (3) definition of some criteria to detect peaks within this window (e.g., a threshold beyond which the SC peak can not be considered significant, see Fig. 2.1). After the identification of peaks, feature extraction can be performed. These features are usually defined through qualitative or semi-quantitative models.

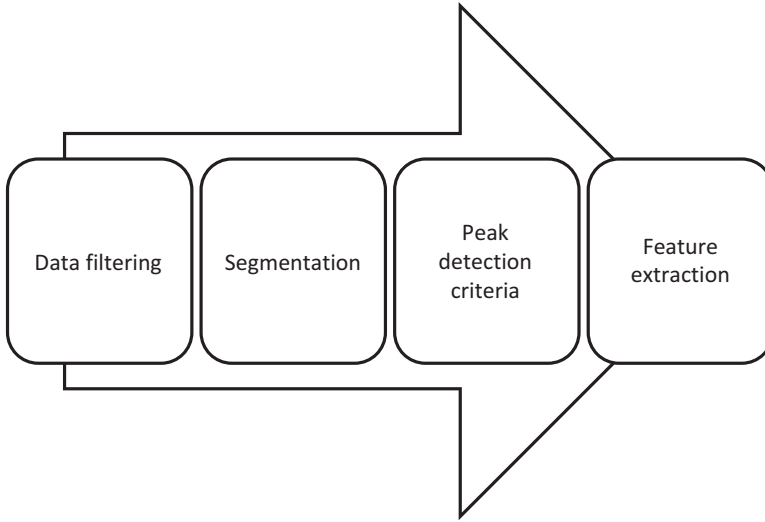


**Fig. 2.1** General diagram of a conventional analysis procedure

### 2.2.2 *Model-Based Approach*

The model-based approach describes how the observable process, i.e., EDA, is generated by the central process, (e.g., sympathetic arousal) using mathematical equations that formulate psychophysiological assumptions. Therefore, the model predicts the SC time series, and the independent variable consists in the unobservable psychological status. However, in the analysis of experimental data we have to consider the opposite situation: we know the observed SC data but not the central state, and we try to estimate the time series of the central process that generated these SC data. To this extent, the forward model has to be turned backwards, to find the relation between SC and central state. In statistics, this mathematical process is often termed “model inversion”. In conclusion, both conventional and model-based analysis try to infer the CNS state from the peripheral signals, but the difference is that model-based methods use a more stringent mathematical language and computational methods to do so, while the general aim is the same [64].

Usually, the model-based methods distinguish two steps in the relationship between the central state and the SC data: the neural model that specifies how the central state, in terms of event-related or spontaneous sympathetic arousal, elicits SMNA, and the peripheral model, from the SMNA to the SC, that specifies how SMNA generates SC usually in the form:

$$SC = SMNA * IRF$$

where  $*$  is the convolution operator, and IRF is a skin conductance impulse response function. This model is, in a basic version, deterministic. Through this approximation, the SC time series is only influenced by SMNA and not by other confounding factors such as noise (note that the deterministic deconvolution enhances noise [16]). Different model inversions schemes treat this problem differently.

### 2.2.2.1 Model Evaluation

The evaluation of a model and the comparison between two or more methods is hard to be performed. Each method returns an output that can be an index or the central state, but we have to measure which method estimates the central state at best. A possible evaluation process uses an experimental paradigm in order to create two central states that are known to be different. Thus, the method can be evaluated investigating the ability to detect this difference. This is achieved using a statistical approach on the features extracted that quantify the central activation.

In this book, we first present a conventional modeling approach, the Continuous Deconvolution Analysis (CDA) [1], and a recently proposed model proposed by Greco et al. based on rigorous mathematical definitions: the convex optimization approach (cvxEDA). In the next chapters, performance of this model will be empirically evaluated and compared.

## 2.3 CDA: Continuous Deconvolution Analysis

The CDA is a method, proposed by Benedek et al., to decompose the skin conductance signal into its tonic and phasic driver data. It is based on an explicit biophysical model, and its parameters are optimised for each individual dataset. The decomposition process comprised in three different steps: a preprocessing phase, in which the signal is filtered to reduce the noise, a deconvolution process in order to obtain the phasic and tonic driver, and an optimization stage to improve the estimation of the parameters of the impulse response function. The decomposition process can be performed by means of the toolbox Ledalab. software package for MATLAB [70], which is available online ([www.ledalab.de](http://www.ledalab.de)).

### 2.3.1 Preprocessing

In the preprocessing stage, the detection of movement artifacts was carried out by visual inspection. Artifact-free signals exclusively were taken into account for further analysis. In order to limit the frequency bandwidth of the EDA signal, it was filtered with a low pass zero-phase forward and reverse digital filter [71, 72] with a cutoff frequency of 2 Hz, having Butterworth approximation.

### 2.3.2 EDA Deconvolution Analysis

EDA is produced by changes in the skin conductivity as major effect of the sweat gland activity. Specifically, sweat is released to the sweat duct, passes to the stratum corneum, and finally is brought out of the skin. Accordingly, the dynamics of the variation of concentration of sweat in the stratum corneum can be represented by a two-compartment pharmacokinetic model in which the sweat concentration is assumed to change only by diffusion [14, 73]. The first compartment represents the sweat duct and the second compartment the stratum corneum. Being the two compartments different in dimension (i.e. the stratum corneum is much larger than the sweat duct), the diffusion can be considered as a one way-diffusion. Solving the two coupled first-order differential equations of each compartment, the solution is the Impulse Response Function  $IRF(t)$  which is also known as Bateman function [74]:

$$IRF(t) = (e^{-\frac{t}{\tau_1}} - e^{-\frac{t}{\tau_2}}) \cdot u(t) \quad (2.1)$$

The Bateman function is characterized by a steep onset and a slow recovery. The steepness of onset and recovery is determined by the time constants  $\tau_1$  and  $\tau_2$ .

EDA can be divided into tonic (SCL: Skin Conductance Level) and phasic components (SCR: Skin Conductance Response). The tonic electrodermal component represents the baseline level of the signal whereas the phasic component indicates a direct response to a specific stimulus. However, there are often phasic parts of EDA which cannot be related to any specific stimulus, and hence, they are called spontaneous or nonspecific SCRs [23]. When the time interval between two consecutive stimuli is shorter than the recovery period of SCR, the stimuli responses in the SCR are overlapped. In this case, the typical shape of the SCR is lost and this could be one of the main issue for the extraction of the correct information from the electrodermal signal. In order to overcome this issue, the EDA signal process is modeled as a convolution process between the SudoMotor Nerve Activity (SMNA), as part of the sympathetic nervous system, and IRF [1] under the hypothesis that EDA is controlled by SMNA resulting in a sequence of distinct impulses which regulate the eccrine sweat glands dynamics (see Fig. 2.2).

Formally, it is possible to write:

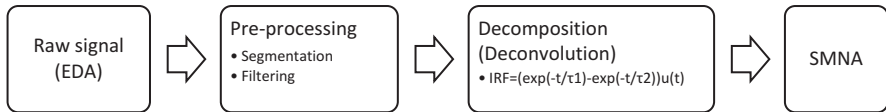


**Fig. 2.2** Electrodermal acquisition and decomposition process. The EDA is filtered to reduce the noise and then decomposed in tonic and phasic components by means of a deconvolution with an impulse response function (IRF) called Bateman function

$$EDA = SMNA \otimes IRF \quad (2.2)$$

where  $SMNA = (DRIVER_{tonic} + DRIVER_{phasic})$ . In the Eq. (2.2), SMNA is unknown and is evaluated by deconvolving the EDA signal with the IRF. To decompose the obtained SMNA signal into the  $DRIVER_{tonic}$  and  $DRIVER_{phasic}$  components, several algorithmic steps should be taken into account. A smoothing Gauss window of 200 ms is applied to SMNA, followed by a peak detection algorithm in order to find the peaks over a threshold of  $0.2 \mu S$ . All the points below the threshold were interpolated with a cubic spline fitting method giving the  $DRIVER_{tonic}$ . More details can be found in [1]. Finally, the  $DRIVER_{phasic}$  component, instead, is computed by subtracting the previously estimated  $DRIVER_{tonic}$  from the SMNA (see Fig. 5.23), under the hypothesis that tonic activity is observed in the absence of any phasic activity [23].

Of note, the  $DRIVER_{phasic}$  signal should have a zero baseline intermitted by distinct peaks overcoming the issue of having overlapped SCRs.

### 2.3.3 Optimization

Starting from fixed values, the parameter set of the IRF (i.e.  $\tau_1$  and  $\tau_2$ ) was optimized according to criteria evaluating the quality of the model, through the minimization of a specific cost function given by the sum of the number of points of the  $DRIVER_{phasic}$  component that have negative value and the number of points above a predefined threshold (equal to 5 % of the maximum of  $DRIVER_{phasic}$ ). This procedure aims at having a signal with a zero baseline a peaks as distinguishable as possible. More details can be again found in [1].

## 2.4 CvxEDA: A Convex Optimization Approach to Electrodermal Activity Processing

CvxEDA has been inspired by some aspects of the CDA model, such as the Batman function. This novel algorithm is based on three main concepts: maximum a posteriori probability, convex optimization, and sparsity.

### 2.4.1 Convex Optimization

A set  $K \in \mathbb{R}^n$  is convex if:

$$\lambda x + (1 - \lambda)y \in K \quad (2.3)$$

$\forall x, y \in K$  and  $\lambda \in [0; 1]$ . A function is convex if:

$$f(\lambda x + (1 - \lambda)y) \leq \lambda f(x) + (1 - \lambda)f(y) \quad (2.4)$$

$\forall x, y \in K$  and  $\lambda \in [0; 1]$ . The meaning of the inequality (2.4) is that, for any two points  $x$  and  $y$  in the domain of the function, the segment between  $(x; f(x))$  and  $(y; f(y))$  lies above the graph of the function. Equivalently, we can define a convex function as a function whose epigraph is a convex set [68].

Considering a standard optimization problem:

$$\begin{aligned} &\text{minimize } f_0(x) \\ &\text{subj. to } f_i(x) \leq 0 \quad i = 1, \dots, m, \end{aligned} \quad (2.5)$$

the optimal choice is the one minimizing the objective function  $f_0(x)$ , which represents the cost of choosing  $x$ , while simultaneously satisfying the constraints  $f_i(x) \leq 0$ . An optimization problem is convex when both the objective and the constraint functions are convex. In the context of mathematical optimization, the most important consequence of convexity is that necessary conditions for local optimality are also sufficient for global optimality. Moreover, important categories of convex optimization problems can be solved efficiently (this is rarely the case for general nonconvex problems).

A special subclass of convex optimization problems is represented by least-square problems where the goal is the unconstrained minimization of a quadratic objective function  $\|Ax - b\|_2^2$ . For this class of problems—frequently arising in regression analysis, parameter estimation and data fitting methods [68]—an analytical solution exists. An important statistical interpretation is that the least-square solution coincides with the maximum likelihood estimation in the case of a linear model corrupted by additive Gaussian noise. Regularization, e.g. adding a norm of the optimization variable  $x$  as an extra term to the cost function, can be applied to least-squares problems to prevent overfitting ( $L_2$ -norm) or to favour sparse solutions ( $L_1$ -norm). While in the former case an analytical solution exists, in the case of the  $L_1$ -regularization the problem can be cast as a quadratic program (QP), i.e. a convex problem with quadratic cost function and affine constraints:

$$\begin{aligned} &\text{minimize } \frac{1}{2} x^T P x + q^T x + r \\ &\text{subj. to } Hx - g \leq 0 \text{ and } Ux - v = 0. \end{aligned} \quad (2.6)$$

### 2.4.2 Model Assumptions

In this model, the EDA generation process based on the following assumptions:



- A1) SCRs are preceded by bursts from the sudomotor nerves controlling the sweat glands. These bursts are temporally discrete episodes [75, 76], i.e. SCRs are generated by a neural signal that is sparse and non-negative because of the nature of a nerve activity.
- A2) The relationship between the number of sweat glands recruited and the amplitude of a firing burst is linear [76]. Moreover, the output response of the system depends only on the instant where the nerve input is applied. Stated otherwise, the timecourse of a single SCR induced by a neural burst is not influenced by previous ones, even when their SCRs overlap [77]. In the light of these considerations it is reasonable to characterize the system as linear time-invariant.
- A3) The sweat diffusion process has a subject-specific impulse response function (IRF) which is relatively stable for all SCRs from the same subject [1].
- A4) This phasic activity is superimposed to a slowly varying tonic activity with spectrum below 0.05 Hz [78], i.e. whose information content can be represented by samples spaced every 10 s (e.g., by 10-s averages in [15]).

### 2.4.3 Observation Model

A given  $N$ -sample long SC signal ( $y$ ) is modeled as the sum of a tonic ( $t$ ) and a phasic ( $r$ ) component plus an additive noise term ( $\epsilon$ ):

$$y = r + t + \epsilon, \quad (2.7)$$

where  $y$ ,  $t$ ,  $r$ , and  $\epsilon$  are  $N$ -long column vectors. The noise term  $\epsilon$  is an iid (independent and identically distributed) sequence of zero-average Gaussian random variables with variance  $\sigma^2$ , representing measurement and modelling errors.

The tonic component is represented as the sum of cubic B-spline functions with equally-spaced knots every 10 s (assumption A4), an offset and a linear trend term:

$$t = B\ell + Cd, \quad (2.8)$$

where  $B$  is a tall matrix whose columns are cubic B-spline basis functions,  $\ell$  is the vector of spline coefficients,  $C$  is a  $N \times 2$  matrix with  $C_{i,1} = 1$  and  $C_{i,2} = i/N$ ,  $d$  is a  $2 \times 1$  vector with the offset and slope coefficients for the linear trend.

Within  $r$ , the shape of a single phasic response (under assumptions A2 and A3) is modelled using a biexponential impulse response function, called the Bateman function:

$$h(\tau) = (e^{-\frac{\tau}{\tau_0}} - e^{-\frac{\tau}{\tau_1}}) u(\tau), \quad (2.9)$$

where  $\tau_0$  and  $\tau_1$  are, respectively, the slow and fast time constants while  $u(\tau)$  is the unitary step function. The Bateman function is the output of a bi-compartmental

pharmacokinetic model representing the diffusion of the sweat through the gland ducts [73]. The Laplace transform of (2.9) is simply:

$$\mathcal{L}\{h(\tau)\} = \frac{1}{s + \tau_0^{-1}} - \frac{1}{s + \tau_1^{-1}}, \quad (2.10)$$

where  $-\tau_0^{-1}$  and  $-\tau_1^{-1}$  are the poles of this second-order LTI system. Its discrete-time approximation, obtained using central differencing (bilinear transform)  $s = \frac{2}{\delta} \frac{z-1}{z+1}$  with sampling interval  $\delta$ , is the following ARMA model:

$$\begin{aligned} H(z) &= \frac{(1 + z^{-1})^2}{\psi + \theta z^{-1} + \zeta z^{-2}} \\ \psi &= (\tau_1^{-1}\delta + 2)(\tau_0^{-1}\delta + 2)/(\tau_1^{-1}\delta^2 - \tau_0^{-1}\delta^2) \\ \theta &= (2\tau_1^{-1}\tau_0^{-1}\delta^2 - 8)/(\tau_1^{-1}\delta^2 - \tau_0^{-1}\delta^2) \\ \zeta &= (\tau_1^{-1}\delta - 2)(\tau_0^{-1}\delta - 2)/(\tau_1^{-1}\delta^2 - \tau_0^{-1}\delta^2). \end{aligned} \quad (2.11)$$

The ARMA cascade can be represented in matrix form as:

$$q = A^{-1}p, \quad r = Mq, \quad (2.12)$$

where:  $p$  represents the sudomotor nerve activity;  $q$  is an auxiliary variable that will be used to find  $p$  indirectly;  $M$  is a tridiagonal matrix with elements  $M_{i,i} = M_{i,i-2} = 1$ ,  $M_{i,i-1} = 2$ ,  $3 \leq i \leq N$ ; and  $A$  is a tridiagonal matrix with elements  $A_{i,i} = \psi$ ,  $A_{i,i-1} = \theta$ ,  $A_{i,i-2} = \zeta$ ,  $3 \leq i \leq N$ .

Finally, the observation model (2.7) can be written as:

$$y = Mq + B\ell + Cd + \epsilon. \quad (2.13)$$

#### 2.4.4 Maximum a Posteriori Estimation

Given the observation model (2.13), the goal is to identify the maximum a posteriori (MAP) spike train ( $p$ ) and tonic component ( $t$ ) parametrized by  $[q, \ell, d]$ , for the measured SC signal ( $y$ ):

$$[q, \ell, d] = \arg \max_{q, \ell, d} P[q, \ell, d | y]. \quad (2.14)$$

Assuming independence between  $q$ ,  $\ell$  and  $d$  (i.e. between the phasic activity, the slowly varying tonic component and the drift) and applying Bayes' theorem, we obtain:

$$P[q, \ell, d | y] \propto P[y | q, \ell, d] P[q] P[\ell] P[d], \quad (2.15)$$

where  $P[y \mid q, \ell, d]$  is the likelihood of observing a specific SC time series given the parameters of the model, while  $P[q]$ ,  $P[\ell]$  and  $P[d]$  are the prior probabilities of the parameters. In (2.15), we omitted the evidence of the SC data  $P[y]$  since it plays no role in the optimization. Unlike other approaches in the literature, our model relies exclusively on the presence and definition of the priors in (2.15)—which we are about to describe in detail—to impose physiologically sound constraints on the signals to be estimated. As a result, the method does not require pre-processing of the observed SC signal (e.g., bandpass filtering) nor post-processing of the inferred phasic and tonic components (e.g., to deal with negative neural activations).

To model the sudomotor nerve activity ( $p$ ) representing the input ( $\mathcal{A}1$ ) to the LTI system, the simplest first order description of spike trains is used [79], i.e. a Poisson distribution:

$$p_i \sim \text{Pois}(\lambda\delta), \quad (2.16)$$

where  $\lambda\delta$  is the expected firing rate per bin, i.e.  $\lambda$  is the average number of spikes per unit time. To keep the analysis tractable, the Poisson distribution is replaced with an exponential distribution of the same mean [79]. In this way the constraint  $p_i \in \mathbb{N}$  can be relaxed to  $p_i \geq 0$ . Finally, since  $p$  and  $q$  are related by (2.12), the prior  $P[q]$  becomes:

$$P[q] = \prod_{i=1}^N \frac{1}{\lambda\delta} e^{-\frac{1}{\lambda\delta} p_i} \propto \prod_{i=1}^N e^{-\frac{1}{\lambda\delta} (Aq)_i}. \quad (2.17)$$

Concerning the tonic component, the authors make use of assumption  $\mathcal{A}4$  and consider a uniform frequency spectrum in the band  $0 - 0.05$  Hz. Because equally-spaced knots every  $\Delta = 10$  s are used, the sampling frequency is exactly twice the upper band limit and the elements of the vector  $\ell$  can be assumed iid. In particular, a normal distribution is adopted for the amplitude at each knot  $\ell_i \sim \mathcal{N}(0, \sigma_\ell^2)$ . As a result the prior  $P[\ell]$  is:

$$P[\ell] = \prod_{i=1}^Q \frac{1}{\sqrt{2\pi} \sigma_\ell} \exp\left(-\frac{1}{2} \frac{\ell_i^2}{\sigma_\ell^2}\right), \quad (2.18)$$

where  $Q$  is the number of knots (approximately  $N\delta/\Delta$ ). Finally, for the drift coefficients  $d$  an uninformative priors is assumed and drop  $P[d]$  altogether from further analysis.

The likelihood term follows immediately from (2.13) and from the error model  $\epsilon \sim \mathcal{N}(0, \sigma^2)$ :

$$P[y \mid q, \ell, d] = \prod_{i=1}^N \frac{1}{\sqrt{2\pi} \sigma} \exp\left(-\frac{(Mq + B\ell + Cd - y)_i^2}{2\sigma^2}\right). \quad (2.19)$$

Replacing (2.17), (2.18) and (2.19) in (2.15) and taking the logarithm:

$$\begin{aligned} \ln P[q, \ell, d | y] = & -\frac{1}{2\sigma^2} \sum_{i=1}^N (Mq + B\ell + Cd - y)_i^2 \\ & - \frac{1}{\lambda\delta} \sum_{i=1}^N (Aq)_i - \frac{1}{2\sigma_\ell^2} \sum_{i=1}^Q \ell_i^2 + \text{const}, \end{aligned} \quad (2.20)$$

with  $(Aq)_i \geq 0$ . Maximizing (2.20) yields the MAP solution to (2.14). After multiplying by  $\sigma^2$  and substituting  $\alpha = \sigma^2/(\lambda\delta)$  and  $\gamma = \sigma^2/\sigma_\ell^2$ , (2.20) is rewritten as a constrained minimization problem in matrix form to obtain a more compact notation. This optimization problem, that is termed cvxEDA, represents the core of the algorithm presented in this manuscript:

$$\begin{aligned} & \text{minimize } \frac{1}{2} \|Mq + B\ell + Cd - y\|_2^2 + \alpha \|Aq\|_1 + \frac{\gamma}{2} \|\ell\|_2^2 \\ & \text{subj. to } Aq \geq 0. \end{aligned} \quad (2.21)$$

After some matrix algebra, this optimization problem can be re-written in the standard QP form and solved efficiently using one of the many sparse-QP solvers available. After finding the optimal  $[q, \ell, d]$ , the tonic component  $t$  can be derived from (2.8) while the sudomotor nerve activity driving the phasic component can be easily found as  $p = Aq$ .

Although solving (2.21) is strictly equivalent to maximizing (2.20), the former has a different interpretation. In the optimization problem, the objective function to be minimized is a quadratic measure of misfit between the predicted and the observed data. Prior knowledge is accounted for by means of additive regularizing terms. For example, the spiking nature of the driving input (assumption  $\mathcal{A1}$ ) is enforced by means of the  $l^1$ -norm penalization which is an effective way to sparsify a signal while maintaining convexity [80–82]. Smoothness of the tonic curve (assumption  $\mathcal{A4}$ ) is enforced by the choice of the basis ( $B$ ) and through the  $l^2$ -norm penalization of the spline coefficients. The two parameters  $\alpha$  and  $\gamma$  control the strength of the penalty for the phasic and tonic components, respectively. A large  $\alpha$  (stronger  $l^1$  regularization of  $p$ ) yields a sparser estimate with most noise-induced spurious spikes suppressed but also more signal distortion (i.e. attenuation of genuine activations). Conversely, a small  $\alpha$  produces a less distorted but noisier solution. Concerning  $\gamma$ , higher values mean a stronger penalization of  $\ell$ , i.e. a smoother tonic curve.

Of note, CvxEDA algorithm is implemented in Matlab language and the software is available online ([www.mathworks.com/matlabcentral/fileexchange/53326-cvxeda](http://www.mathworks.com/matlabcentral/fileexchange/53326-cvxeda)).

## 2.5 Feature Extraction

Regardless of the model or the type of analysis used to perform the decomposition of the EDA signal, several features are extracted from tonic and phasic signals in order to assess the sympathetic system activity.

### 2.5.1 Time Domain

Typically, time-domain features of EDA are widely used to quantify the overall activation of the ANS. Features extracted from the phasic signal are usually calculated into time windows of 5 s after the onset of the external stimulus (according to the knowledge that SCRs arise within 1–5 s after the stimulus onset [16, 83]). Features extracted from the tonic component express the sympathetic tone and are often computed within time windows of 20 s, since the upper cut-off frequency of the tonic component is about 0.05 Hz [84]. Moreover, within the group of tonic measurements, nonspecific skin conductance responses are included, by definition. They are often characterized by their frequency and mean amplitude within the time window analysis.

In Table 2.1, the features set is summarized along with the corresponding description.

**Table 2.1** List of the features extracted from the EDA phasic and tonic components

| Feature     | Description   |
|-------------|---|
| nSCR        | Number of significant SCRs within the time response windows (WTRW) of 5 s |
| MAX-Tonic   | Maximum value of the tonic curve within the time window                   |
| MAX-Phasic  | Maximum value of the phasic curve WTRW                                    |
| AUC-Tonic   | Area under the tonic curve over time                                      |
| AUC-Phasic  | Area under the phasic curve WTRW  |
| Mean-Tonic  | Mean value of the tonic component over time                               |
| Mean-Phasic | Mean value of the phasic component WTRW                                   |
| STD-Tonic   | Standard deviation of the tonic component                                 |
| STD-Phasic  | Standard deviation of the phasic component WTRW                           |
| NsSCR freq  | Frequency of the NsSCRs   |
| Mean-NsSCR  | Mean value of the NsSCRs component over time                              |

### 2.5.2 *Frequency Domain*

In addition to the features defined in the time domain, recently Posada-Quintero et al. [85] proposed an analysis of the Power Spectral Density (PSD) of the EDA signal in order to assess the sympathetic nervous system activity.

The effective assessment of the sympathetic dynamics, in fact, can have important diagnostic impact and is one of the major fields of interest in cardiovascular research [86]. The most common way to assess the ANS dynamics is to compute the PSD of the HRV [87]. The HRV spectrum can be considered as characterized by three components: the high-frequency (HF) bandwidth, from 0.15 to 0.4 Hz, that is known to be influenced only by the parasympathetic nervous system activity; low frequency (LF) bandwidth, from 0.045 to 0.15 Hz, which is influenced by both the sympathetic and parasympathetic nervous system activities, and the very low frequency (VLF) from 0.0033 to 0.04 Hz. Therefore the ratio between LF and HF, which was typically used to assess the ANS balance, is not fully accepted as an accurate measure of the balance between sympathetic and parasympathetic systems, since the LF band also contains parasympathetic dynamics.

Thus, since EDA is directly controlled only by the sympathetic branch of the ANS, Posada-Quintero et al. examined if a similar association of LF components of HRV to sympathetic function also exists with the sudomotor function as measured by EDA. In fact, in this way the main disadvantage of LF domain analysis of HRV could be overcome because EDA is not influenced by the parasympathetic nervous system activity.

In their study, Posada-Quintero et al., considered only tonic and NsSCRs, since they were mainly interested in tonic stress responses, and excluded from the analysis the evoked SCR. The time-domain parameters of the tonic components, such as the tonic mean value as well as the NsSCRs frequency (see Fig. 2.3), are strictly related to the sympathetic activity but these indices are highly variable among subjects [88]. Therefore, they have calculated the PSD of the EDA (see Fig. 2.3) investigating the assumption that, if EDA can represent the cardiac and peripheral sympathetic nervous systems dynamics, the spectral power should be largely present in the low frequency band (0.04–0.15 Hz). Actually, after three experimental paradigms concerning orthostatic, physical and cognitive stress, they concluded that the frequency response of the sympathetic activities represented in the EDA signal can be defined to be within 0.045–0.25 Hz. In addition, analyzing EDA in the frequency domain, the PSD can lead to less inter-subject variability as compared to the tonic features defined in the time domain (which are known to be reliable indices of the overall sympathetic activation), due to the inherent filtering properties of the frequency domain transformations. Finally, as stated above, the EDA represents only the sympathetic nervous activities, whereas the LF power of the HRV comprises both parasympathetic and sympathetic activities. Therefore, thanks to the analysis in the frequency domain, it is possible to obtain a marker of the sympathetic activity, which can be considered more reliable and sensitive than the LF power of HRV.

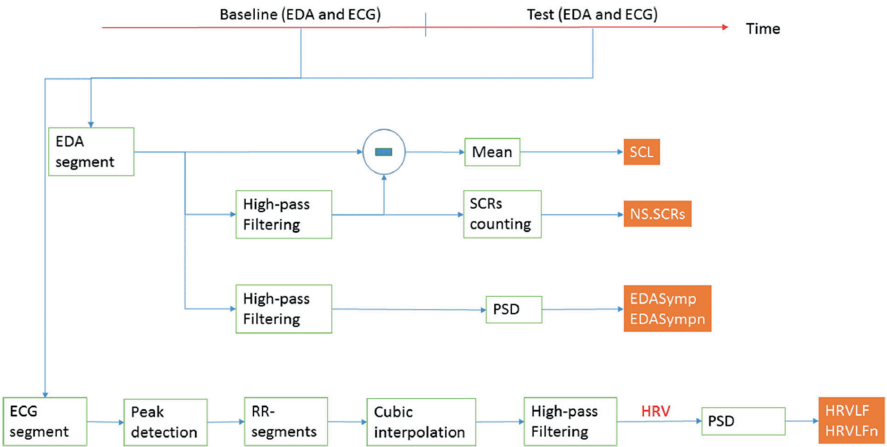


**Fig. 2.3** Diagram of the signal processing procedure to extract EDA and HRV parameters. Courteously from [85]





Advances in Electrodermal Activity Processing with  
Applications for Mental Health

From Heuristic Methods to Convex Optimization

Greco, A.; Valenza, G.; Scilingo, E.P.

2016, XVIII, 138 p. 51 illus., 22 illus. in color., Hardcover

ISBN: 978-3-319-46704-7